Spurious Solutions in the Multiband Effective Mass Theory Applied to Low Dimensional Nanostructures*

B. Lassen[1], R.V.N. Melnik[1,2] and M. Willatzen[1]

[1] The Mads Clausen Institute, The University of Southern Denmark,
DK-6400, Denmark

[2] M^{2}NeT Lab, Wilfrid Laurier University,
75 University Avenue West, Waterloo, Ontario N2L 3C5, Canada

Abstract

In this paper we analyze a long standing problem of the appearance of spurious, non-physical solutions arising in the application of the effective mass theory to low dimensional nanostructures. The theory results in a system of coupled eigenvalue PDEs that is usually supplemented by interface boundary conditions that can be derived from a variational formulation of the problem. We analyze such a system for the envelope functions and show that a failure to restrict their Fourier expansion coefficients to small k components would lead to the appearance of non-physical solutions. We survey the existing methodologies to eliminate this difficulty and discuss a simple and effective solution. This solution is demonstrated on an example of a two-band model for both bulk materials and low-dimensional nanostructures. Finally, based on the above requirement of small k, we derive a model for nanostructures with cylindrical symmetry.

Keywords: Effective envelope theory, abrupt interfaces, plane wave approximations, k space, Fourier coefficients, variational formulation, interface boundary conditions, band gap, spurious solutions, low dimensional semiconductor nanostructures

1   Introduction

The electronic structure calculation is among the most fundamental problems in modern science and engineering. While achieving a higher accuracy in the methods for such calculations remains an important issue, our ability to construct simpler computational algorithms that would allow us to obtain reliable results in a more efficient and cost-effective manner is paramount for our progress at the practical level with far reaching ramifications in technological applications.

From a mathematical point of view, most methodologies for the construction of such algorithms are based on effective theories where we attempt to reduce the degrees of freedom

---

and to bridge modelling scales [27, 26]. One such theory, derived with the application of the effective mass theorem [32] and known as the multiband effective mass approximation, provides a fundamental tool in predicting electronic properties of structures. We are interested in the development of an efficient computational tool for predicting electronic properties of quantum heterostructures, that is the low-dimensional (semiconductor) nanostructures where the motion of electrons is restricted, forcing them into a quantum confinement [37]. Examples of such structures include quantum wells, quantum wires, or quantum dots, where the motion of electrons is restricted in one, two, or all three directions, respectively. Properties of these small nanocrystals, containing often from a few hundred to a few thousand atoms, are very different from the same material in bulk, which results in a wide range of their current and potential applications, from biological tags for proteins to applications in quantum computing, and to a new generation of optoelectronic devices.

The reason for such an undertaking stems from the fact that typical characteristic dimensions of nanostructures is ranging between 1 to 100 nm while the characteristic dimensions of atoms are between 0.1 to 0.7nm. As a result, in many situations of dealing with nanostructures, atomistic approaches become not only unpractical, but often prohibitive. This is particularly true when we have to account for a multiscale nature of the problem (e.g., [25, 20]) and its multiphysics character where several physical fields, such as mechanical and electric, act simultaneously (e.g., [38, 27]).

In dealing with (nano)crystals we use the fact of crystal symmetry characterized by the transformations which in the bulk case leave the structure, and hence its Hamiltonian (the energy operator), invariant. As explained in the Appendix, the representations of the translation group are characterized by a vector $\mathbf{k}$ in the first Brillouin zone of the crystal. The relevance of the $\mathbf{k}$ vector is clearly seen from the Bloch theorem, stating that any solution for a periodic structure (bulk material) can be represented in the form:

$$\psi_{n\mathbf{k}}(\mathbf{r}) = \exp(i\mathbf{k}\mathbf{r})U_{n\mathbf{k}}(\mathbf{r}), \tag{1}$$

where $U_{n\mathbf{k}}$ has the given periodicity. The n in Eq. (1) reflects a multiband nature of the energy operator spectrum and the basic task in the $\mathbf{k}$-space can be formulated as the determination of this spectrum throughout one Brillouin zone (usually, the first Brillouin zone, see Appendix). In the case of a nanocrystal this theorem does not apply anymore. Instead, the wave function can be expanded in terms of Bloch solutions:

$$\psi(\mathbf{r}) = \sum_n \int c_n(\mathbf{k}) \exp(i\mathbf{k}\mathbf{r})U_{n\mathbf{k}}(\mathbf{r})d^3k, \tag{2}$$

where the integral is over the first Brillouin zone. It turns out that it is advantageous to rewrite the expansion in term of a specific set of periodic solutions, and the zone-center solutions U_{n0} are usually chosen for this purpose. Hence, by using $U_{n\mathbf{k}}(\mathbf{r}) = \sum_{n'} d_{nn'}(\mathbf{k})U_{n'0}(\mathbf{r})$, we get:

$$\psi(\mathbf{r}) = \sum_n \int \tilde{F}_n(\mathbf{k}) \exp(i\mathbf{k}\mathbf{r})d^3k U_{n0}(\mathbf{r}) = \sum_n F_n(\mathbf{r})U_{n0}(\mathbf{r}), \tag{3}$$

where $\tilde{F}_n(\mathbf{k}) = \sum_{n'} c_{n'}(\mathbf{k})d_{n'n}(\mathbf{k})$. The idea of the envelope function (EF) based on the representation (3) is a key to a substantial simplification of the original problem in determining properties of the heterostructures. This representation leads to a major advantage of the EF multiband effective mass methodologies compared to computationally intensive

ab initio and atomistic approaches and allows us to extend the energy-band theory beyond perfectly periodic crystals. Known for bulk materials since 50-ies (e.g., [24, 1, 31, 9]), this methodology has successfully been extended to situations that allow us to treat efficiently lattice-mismatched heterostructures where we frequently have to deal with two (or more) materials with different properties, both theoretically and computationally [3, 4, 11, 5, 19]. One of the main difficulties in implementing multiband effective mass models is the appearance of spurious solutions. Although these solutions are correct solutions of the multiband model in question, they have nothing to do with the physics of the problem as they are not solutions to the original problem (e.g., [21, 22]).

The goal of this paper is two fold. First, we want to highlight the reason for the appearance of spurious solutions using a simple one dimensional two band model and give an overview of different approaches for the removal of spurious solutions. Second, within one of the approaches, the so-called cut-off method, we show how additional symmetries can be taken into account. More specifically, we show how a three dimensional cylindrical symmetric problem can be simplified.

The structure of the rest of the paper is as follows. In the next section we explain the main difficulties in applying the effective mass theory to the analysis of nanostructures and provide an overview of existing methodologies directed to the elimination of spurious solutions. In this section we also provide the reader with a brief discussion of the main approaches in this field to the treatment of interface boundary conditions. In Section 3 we give details of the basic model obtained from the generalized envelope function theory in one dimension, followed by two examples. The first example is concerned with a stepwise constant crystal potential and deal with the bulk situation. The second example is concerned with the treatment of a heterostructure where we have to deal with abrupt interface conditions. This example demonstrates difficulties in the application of the envelope function theory in practice, connected with the spurious solution phenomenon. We highlight the physical roots of this problem and a computational procedure to circumvent arising difficulties. In Section 4 we demonstrate this procedure on an example of cylindrically symmetric systems. Conclusions and future directions are presented in Section 5.

2 Interface boundary conditions, spurious solutions, and existing methodologies

As a framework for the discussion we show in Fig. 1 a schematic representation of a nanoscale heterostructure. The first question that arises in the context of the model we are considering here is about the regularity of the envelope function at the interface (the abrupt hetero-junction), in particular whether this function is continuous or discontinuous. If the Fourier components of the envelope function are clustered around the center of the interval where the problem is considered, then the model is reducible to the standard Sturm-Liouville eigenvalue problem for the second order differential operator. Otherwise, a higher order model needs to be considered. Connection rules (or the interface boundary conditions) are needed to link the solutions from two different regions at the interface. Such rules can be continuous and represented by certain phenomenological conditions with empirical coefficients that play the role of material parameters characterizing the interface [34] or discontinuous, in agreement with traditional concepts. In the first case, the regularity of the envelope function must be
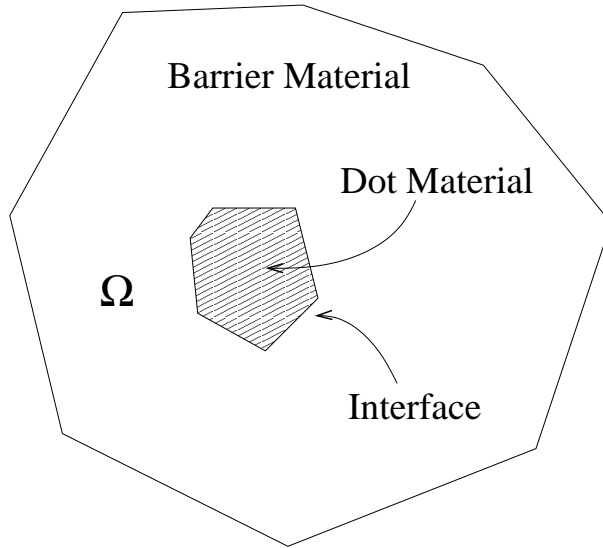
Figure 1: Schematic picture of a nanoscale heterostructure.

relaxed. In the second case, we usually use bulk properties for an extrapolation across the interface defining the connection rules which are in this case discontinuous with the interface width of the order of a lattice constant [13]. Both cases are physically equivalent. Furthermore, the envelope-function theory can be applied to the analysis of nanostructures even in the latter case [4, 11, 6]. According to this theory, the solution to the eigenvalue PDE problem

$$H\mathbf{F} = E\mathbf{F} \tag{4}$$

with H being the effective mass Hamiltonian can be represented in terms of momentum matrix elements and band gaps, including the interfaces. This is shown by deriving a set of integro-differential equations for envelope functions and restricting our attention to the behavior of such functions on the scale larger than the lattice constant by neglecting nonlocal terms. From an experimental point of view, even in the case of large lattice mismatches, many nanostructures, including nanowire heterostructures, exhibit defect-free interfaces [10], making such an assumption well justified. In the general case, the validity of such an approximation in a narrow region near the interface requires, strictly speaking, linking the proposed approach to atomistic methodologies. Another approach, based on an averaging procedure around the interface and valid to the order of around 1Å (the distance between interface atoms) was proposed in [33]. It is important to emphasize here that the problem of formulating correct interface boundary conditions is not limited to the effective mass theory and is debated in the literature in the context of other models in the multiscale hierarchy of mathematical models for nanostructures, e.g. for pseudopotential-based models as well as for tight-binding models [23]. As mentioned, the physical reason behind this debate is the fact that the internal structure of the heterointerface cannot be represented in terms of bulk parameters [34]. This fact and the required reparametrization due to necessary fittings to experimental data may lead to non-trivial difficulties in the formulation of model (4) satisfying ellipticity properties [35]. On the other hand, it is exactly the internal structure of the heterointerface that leads to unique properties of such nanostructures and lend them wide applicability. Several recent approaches have been proposed to overcome the problem

in the context of the effective mass theory based on additional requirements. For example, in [29] the authors used the conservation property of probability density to derive boundary conditions for the envelope functions from the conservation of the current normal to the interface. The derivation of the variational principle for the effective mass theory model has recently been discussed in [30] where phenomenological parameters, in addition to the bulk parameters, are required for the implementation.

An accurate fit to all experimental effective masses in the multi-band effective mass Hamiltonian H from model (4) may lead to spurious, non-physical solutions that contradict one of the most fundamental physical observations, the existence of a band gap in these semiconductor materials. It is a long standing problem known from the literature for quite some time [36]. If we do retain all solutions, there are repeated arguments in the literature that spurious bands have negligible effect on the bound-state eigenfunction properties, but it has been shown that this methodology may lead to the results that contradict physical observations [12]. The premises of the effective mass theory lies with the fact that the model Hamiltonian is accurate in the vicinity of $k = 0$. Therefore, the main ideas for eliminating spurious solutions should rely either on the manipulations with higher order terms k^2 in the Hamiltonian [18], modifying the model, or on rejecting the larger-k solutions as unphysical from the outset [17]. The first approach is not as easy to implement in practice as we might think, e.g. Hamiltonian modifications should remain invariant with respect to symmetry operations of the corresponding groups. In what follows, we base our discussion on the second approach. Before proceeding further, we mention that for efficient practical implementations it is important also to choose a basis that is a good approximation to the Bloch waves of the bulk materials the nanostructure is made of. This can be achieved in several different ways. For example, we can use an averaging procedure around the interface valid to the order of the distance between interface atoms and maintain the continuity of the envelope function as we mentioned before [33]. Alternatively, we can keep the discontinuity across the interface defining it via the connection rules and choose an appropriate basis (by choosing appropriate transformation parameters) such that spurious unphysical solutions are eliminated [12, 14]. The latter methodology has several advantages. For example, the matrix of the resulting system of linear equations under this approach is sparse allowing an efficient computational implementation. This methodology requires an additional assumption on operator ordering in the Hamiltonian.

3 Multiband effective mass theory in one dimension

Consider the eigenvalue PDE problem (4) for a one dimensional crystalline heterostructure described by the following Hamiltonian:

$$H = -\frac{\hbar^2}{2m}\frac{\partial^2}{\partial x^2} + V(x), \tag{5}$$

in some region $\Omega \subseteq \mathbb{R}$ (see Fig. 1), where m is the free electron mass, $\hbar = h/(2\pi)$, and h is Planck's constant. In this case, the two length scales mentioned in the introduction, i.e., the atomistic and the heterostructure scales, are contained within the potential $V(x)$, see section 3.2 for an example. The idea behind k·p theory is to replace one of these length scales, namely the atomistic scale, with material specific parameters. In this paper we use the envelope function theory developed by Burt [4] to achieve this.

Following [3] we start by expanding the wave function ψ in a complete set of periodic and orthonormal functions U_n:

$$\psi = \sum_n F_n(x)U_n(x), \tag{6}$$

where

$$F_n(x) = \int_{-\pi/a}^{\pi/a} \tilde{F}_n(k)e^{ikx}dk, \tag{7}$$

and a is the length of the period. The completeness of the set U_n only relates to functions with the given periodicity. In effective mass theory the periodicity is usually given by the principal lattice cell although this need not be the case. The Fourier expansion is restricted to the first Brillouin zone only because this ensures uniqueness of the envelope functions F_n as is seen from the expansion in periodic Bloch functions in Eq. 2 (the first Brillouin zone is in the one dimensional case given by the interval $]-\pi/a, \pi/a]$). The usual choice of basis is the zone-center solutions U_{n0} as indicated in section 2. Based on this expansion the following infinite set of coupled differential equations can be derived for the envelope functions [3]:

$$-\frac{\hbar^2}{2m}\frac{\partial^2 F_n}{\partial x^2}(x) + \sum_{n'} \frac{-i\hbar}{m}p_{nn'}\frac{\partial F_{n'}}{\partial x}(x) + \sum_{n'} \int_\Omega H_{nn'}(x, x')F_n(x')dx' = EF_n(x), \tag{8}$$

where

$$p_{nn'} = -i\hbar \int_{\Omega_a} U_n^*(x)\frac{\partial U_{n'}}{\partial x}(x)dx, \tag{9}$$

$$H_{nn'}(x, x') = K_{nn'}\delta(x - x') + V_{nn'}(x, x'), \tag{10}$$

$$K_{nn'} = -\frac{\hbar^2}{2m}\int_{\Omega_a} U_n^*(x)\frac{\partial^2 U_{n'}}{\partial x^2}(x)dx, \tag{11}$$

$$V_{nn'}(x, x') = aU_n^*(x')V(x')U_{n'}(x')\Delta(x - x'), \tag{12}$$

$$\Delta(x) = \frac{1}{2\pi}\int_{-\pi/a}^{\pi/a} e^{ikx}dk. \tag{13}$$

Here Ω_a denotes the region of one period, e.g., $]0, a]$. It is worth noting that the non-local term (the last term on the right of Eq. (8)) is a direct consequence of the first Brillouin zone cut-off. This is most easily seen by writing the set of equations in k-space instead of real space:

$$\frac{\hbar^2}{2m}k^2\tilde{F}_n(k) + \sum_{n'} \frac{\hbar}{m}p_{nn'}k\tilde{F}_{n'}(k) + \sum_{n'} \int_{-\pi/a}^{\pi/a} \tilde{H}_{nn'}(k - k')\tilde{F}_n(k')dk' = E\tilde{F}_n(k), \tag{14}$$

where

$$\tilde{H}_{nn'}(k - k') = K_{nn'}\delta(k - k') + \frac{a}{2\pi}\int_\Omega U_n^*(x)V(x)U_{n'}(x)e^{-i(k-k')x}dx. \tag{15}$$

If the integral in the third term on the left of Eq. (14) was not restricted to the first Brillouin zone the equations would be local in real space.

Either of these infinite sets of equations (Eq. (8) or Eq. (14)) can not be solved in general so we need to reduce the infinite set to a finite set of equations. This can in principle be

achieved by finding a unitary operator U which block diagonalizes the problem. To be more specific, let us write Eq. (14) in a slightly different form:

$$\int_{-\pi/a}^{\pi/a} \hat{H}_{nn'}(k,k')\tilde{F}_{n'}(k')dk' = E\tilde{F}_n(k), \tag{16}$$

where

$$\hat{H}_{nn'}(k,k') = \left[\frac{\hbar^2}{2m}k^2\delta_{nn'} + \frac{\hbar}{m}p_{nn'}k\right]\delta(k-k') + \tilde{H}_{nn'}(k-k'). \tag{17}$$

We now divide the set U_n into two groups, a finite group denoted A which we want to solve for, and the rest we denote with R, these are called remote bands. We want to find a unitary operator U so that $\overline{H}_{nn'}(k,k') = [U^\dagger \hat{H}U]_{nn'}(k,k') = 0$ for all k,k' whenever $U_n \in A$ and $U_{n'} \in R$, where operator multiplication is given by:

$$[MN]_{nn'}(k,k') = \sum_l \int_{-\pi/a}^{\pi/a} M_{nl}(k,k'')N_{ln'}(k'',k')dk''. \tag{18}$$

We assume that $[MN]_{nn'}(k,k') < \infty$ for all n,n' and k,k'. In section 3.2 we give an example where this requirement is easily seen to be fulfilled. Under the assumption that such a unitary matrix U exists we can reduce the problem to a finite set of equations. Although it is impossible in generally to find U, this procedure suggests an approximation scheme. We first write U in terms of an operator S given so that $U = e^S$. We then expand S in terms of a power series with respect to a part of $\hat{H}$ assumed to be small. More specifically, we split $\hat{H}$ into two parts, a part assumed to be the main part of $\hat{H}$:

$$\hat{H}_{nn'}^0(k,k') = \tilde{H}_{nn}(0)\delta_{nn'}\delta(k-k'), \tag{19}$$

and the rest $\hat{H}_{nn'}^1(k,k') = \hat{H}_{nn'}(k,k') - \hat{H}_{nn'}^0(k,k')$ is assumed to be small compared to $\hat{H}_0$. For each specific application it is important to verify that $\hat{H}^1$ is indeed small compared to $\hat{H}^0$. This turns out to be the root of the problem with spurious solutions. We will come back to this in section 3.2. Now, we expand around the center of the first Brillouin zone. We then write S as:

$$S = S^1 + S^2 + S^3 + \cdots, \tag{20}$$

where S^i is of order i with respect to elements of $\hat{H}^1$. Using

$$e^{-S}He^S = H + [H,S] + \frac{1}{2}[[H,S],S] + \cdots, \tag{21}$$

we can write $\overline{H}$ in terms of S^i collecting terms of a given order in $\hat{H}^1$, e.g., to the second order in $\hat{H}^1$:

$$\overline{H} = \hat{H}^0 + \hat{H}^1 + [\hat{H}^0, S^1] + [\hat{H}^1, S^1] + [\hat{H}^0, S^2] + \frac{1}{2}[[\hat{H}^0, S^1], S^1] + \cdots. \tag{22}$$

We can now choose S^1 so that $\overline{H}$ is block diagonal to the second order in $\hat{H}^1$, i.e., we choose S^1 so that:

$$[\hat{H}^0, S^1]_{nn'} = -\hat{H}_{nn'}^1, \tag{23}$$
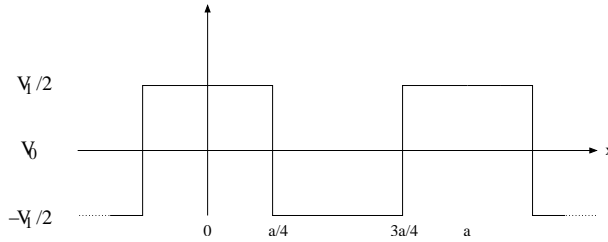
Figure 2: Bulk potential.

for $U_n \in A$ and $U_{n'} \in R$, i.e.,

$$S^1_{nn'}(k, k') = \begin{cases} \frac{\hat{H}^1_{nn'}(k,k')}{\tilde{H}_{n'n'}(0) - \tilde{H}_{nn}(0)} & \text{for } U_n \in A \text{ and } U_{n'} \in R \\ 0 & \text{else.} \end{cases} \tag{24}$$

We then choose S^2 so that $\overline{H}$ is block diagonal to third orders in $\hat{H}^1$ and so on. Using this procedure we can reduce the problem to the finite set A to any order in $\hat{H}^1$. It is usual to disregard terms of third and higher orders in $\hat{H}^1$ resulting in the following set of equations:

$$\begin{aligned} \overline{H}_{nn'}(k, k') &= \left[\frac{\hbar^2}{2m} k^2 \delta_{nn'} + \frac{\hbar}{m} p_{nn'} k \right] \delta(k - k') + \tilde{H}_{nn'}(k - k') \\ &+ \frac{1}{2} \sum_{r \in R} \left(\frac{1}{\tilde{H}_{nn}(0) - \tilde{H}_{rr}(0)} + \frac{1}{\tilde{H}_{n'n'}(0) - \tilde{H}_{rr}(0)} \right) \int_{-\pi/a}^{\pi/a} \hat{H}^1_{nr}(k, k'') \hat{H}^1_{rn}(k'', k') dk'', \end{aligned} \tag{25}$$

for $U_n, U_{n'} \in A$, where $r \in R$ stands for $U_r \in R$. This type of equations are called multiband equations although they are usually formulated in the form of PDEs, see section 3.2.

We now give two examples. In the first example we study bulk properties, i.e., we study the simple situation where the potential is periodic. This serves as a good test example for the application of mulitband equations as the results can be compared to exact (semi-analytical) solutions. It also serves as a framework for more difficult problem with heterostructures. In the second example we investigate a heterostructure for the explicit purpose of showing why spurious solutions appear. We also provide an example of how such spurious solutions can be removed.

3.1   Stepwise Constant Crystal Potential in the Bulk Case

Let us study the case where we have a completely periodic potential $V(x)$ given by a stepwise constant potential (Fig. 2):

$$V(x) = V_0 + V_1 \theta(x), \tag{26}$$

where

$$\theta(x) = \begin{cases} -\frac{1}{2} & \text{for } \frac{a}{4} < x < \frac{3a}{4} \\ \frac{1}{2} & \text{else} \end{cases} \tag{27}$$

for $x \in [0, a]$ and then repeated throughout $\mathbb{R}$, i.e., in this example $\Omega = \mathbb{R}$. The problem can in this case be solved semi-analytically in the sense that the solutions are given by zeros of a transcendental function. The exact solutions are found by using Bloch's theorem which states that solutions are given by $e^{ikx} U_{nk}(x)$ where $U_{nk}(x)$ are periodic solutions to the equation:

$$-\frac{\hbar^2}{2m} \frac{\partial^2 U_{nk}}{\partial x^2}(x) - \frac{i\hbar^2}{m} k \frac{\partial U_{nk}}{\partial x}(x) + \frac{\hbar^2}{2m} k^2 U_{nk} + V(x) U_{kn}(x) = E_{nk} U_{nk}. \tag{28}$$
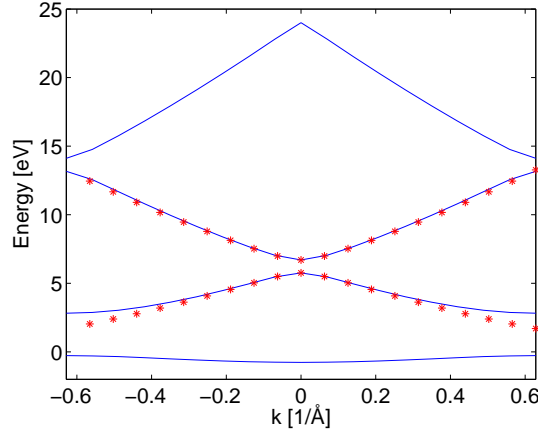
Figure 3: The solid lines show the three first exact dispersion curves and the dots show the dispersion curves found using the two band model. All results are with $V_0 = 0$ eV, $V = 5$ eV and $a = 5$ Å.

This equation can easily be solved by setting up a set of linear equations for the coefficients of the general solutions $e^{\pm i k_i x}$ in each region with constant potential resulting in a transcendental equation for the energies E_{nk}. In Fig. 3 we show the band structure for a specific example, i.e., a plot showing eigen energies as a function of k.

Although we can easily find the exact solutions to this problem, there is still a lot to be learned by applying the above method. In the case of a periodic potential Eq. (15) reduces to:

$$\tilde{H}_{nn'}(k - k') = \delta(k - k') \int_0^a U_n^*(x) H U_{n'}(x) dx. \tag{29}$$

This suggests that periodic zone center eigen solutions to H will be a good choice for the periodic basis , i.e., $U_n = U_{n0}$. With this choice $\tilde{H}_{nn'}(k, k')$ is diagonal and the diagonal elements are given by the periodic eigen energies, i.e.,

$$\tilde{H}_{nn'}(k - k') = E_{n0} \delta_{nn'} \delta(k - k'), \tag{30}$$

and

$$\hat{H}^1_{nn'}(k, k') = \left[\frac{\hbar^2}{2m} k^2 \delta_{nn'} + \frac{\hbar}{m} p_{nn'} k \right] \delta(k - k'). \tag{31}$$

It is clear from this that the elements of $\hat{H}^1_{nn'}$ will be small as long as k is small. In the general case, the question of how small is a currently unresolved non trivial issue. A rule of thumb is that k should be within the first 20% of the first Brillouin zone. Using Eq. (31), the multiband equation Eq. (25) takes on the simple form:

$$\overline{H}_{nn'}(k, k') = \left[\frac{\hbar^2}{2m} \gamma_{nn'} k^2 + \frac{\hbar}{m} p_{nn'} k + E_{n0} \delta_{nn'} \right] \delta(k - k'), \tag{32}$$

where

$$\gamma_{nn'} = \delta_{nn'} + \frac{1}{m} \sum_{r \in R} p_{nr} p_{rn} \left(\frac{1}{E_{n0} - E_{r0}} + \frac{1}{E_{n'0} - E_{r0}} \right). \tag{33}$$
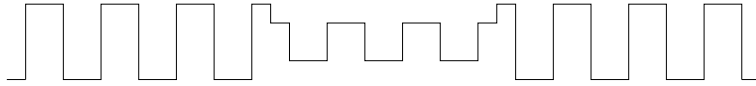
Figure 4: An example of the potential of a heterostructure.

If we choose the second and third zone center solutions, i.e., U_{20} and U_{30} from Eq. (28), as our set A we get:

$$
\begin{pmatrix} \frac{\hbar^2}{2m}\gamma_{22}k^2 + E_{20} & \frac{\hbar}{m}p_{23}k \\ \frac{\hbar}{m}p_{32}k & \frac{\hbar^2}{2m}\gamma_{33}k^2 + E_{30} \end{pmatrix} \begin{pmatrix} \tilde{F}_2(k) \\ \tilde{F}_3(k) \end{pmatrix} = E \begin{pmatrix} \tilde{F}_2(k) \\ \tilde{F}_3(k) \end{pmatrix}.
\tag{34}
$$

This would correspond to the valence and conduction band in a semiconductor. The above multiband equation has the solutions:

$$
\begin{aligned}
E(k) &= \frac{1}{2}\left(\frac{\hbar^2}{2m}(\gamma_{22} + \gamma_{33})k^2 + E_{20} + E_{30} \right) \\
&\quad \pm \frac{1}{2}\sqrt{\left(\frac{\hbar^2}{2m}(\gamma_{22} - \gamma_{33})k^2 + E_{20} - E_{30} \right)^2 - 4\frac{\hbar^2}{m^2}p_{23}p_{32}k^2}.
\end{aligned}
\tag{35}
$$

From the dispersion curves in Fig. 3 we see that the two band model is quite accurate within most of the first Brillouin zone, although this is by no means always the case, see for example [14]. Note also that it is not generally possible to evaluate the infinite sum in Eq. (33), so we truncate it to a sufficient set of remote bands (elements of R). Usually we do not need to include that many remote bands as the denominator ensures that we can disregard remote bands sufficiently far away in energy from the energies of the set A.

3.2   Heterostructure Example

In this section we study the example of a heterostructure consisting of N_b periods of one material, called the barrier material, and N_w periods of another material, called the well material, i.e., the potential is given by:

$$
V(x) = (1 - \theta_h(x))V_b(x) + \theta_h(x)V_w(x),
\tag{36}
$$

where $V_b(x)$ and $V_w(x)$ are bulk potentials with different V_0 and V values but the same period length a and

$$
\theta_h(x) = \begin{cases} 1 & \text{for } -aN_b/2 < x < aN_b/2 \\ 0 & \text{else} \end{cases},
\tag{37}
$$

for $x \in [-a(N_b + N_w)/2, a(N_b + N_w)/2]$, see Fig. 4 for an example. We impose periodic boundary conditions on the outside of our structure, i.e., we extend V to $\Omega = \mathbb{R}$ periodically and impose $F_n(x + NL) = F_n(x)$ for all $N = \mathbb{Z}$, where $L = a(N_b + N_w)$. Alternatively, we could use Dirichlet boundary conditions, however, we are mainly interested in bound states and they are unaffected (or weakly affected) by boundary conditions sufficiently far away from the well region. We use periodic boundary conditions because they are natural for periodic structures as they would insure translational invariance.
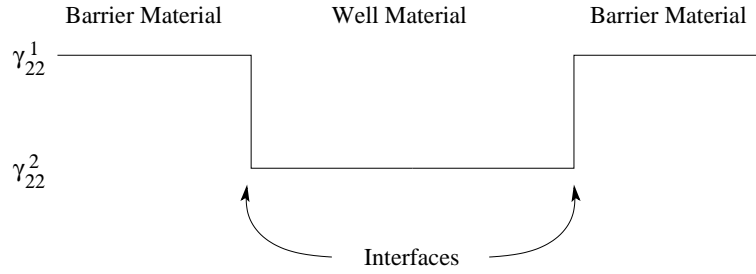
Figure 5: A schematic picture showing the spatial dependence of γ_{22}.

3.2.1   k·p Theory in Practice and the Appearance of Spurious Solutions

One of the major reasons for using k·p theory is to be able to use bulk values also in the case of a heterostructure. The bulk parameters are much easier to determine (either by ab initio calculations or experiments) than parameters appearing in the equations for a heterostructure derived above. Also, if bulk parameters can be used, we do not need to determine heterostructure parameters for each specific structure. For this reason, we would like to treat each material as a bulk material. This corresponds to working with different sets of periodic bases for each material and, as a result, the derivation of multiband equations needs to be modified, see [16]. Alternatively, bulk multiband models for the different materials can be used and connected via interface boundary conditions as discussed in section 2. Which interface boundary conditions to use is still an active area of research and we do not enter this discussion here. Instead, we choose to use interface boundary conditions found using a symmetrization procedure as they serve to highlight why spurious solutions appear.

The multiband equation that we use is given by:

$$\sum_{n'} \left[-\frac{\hbar^2}{2m}\frac{\partial}{\partial x}\left(\gamma_{nn'}(x)\frac{\partial}{\partial x}\right) - i\frac{\hbar}{m}\left(\delta_{n<n'}p_{nn'}(x)\frac{\partial}{\partial x} + \delta_{n'<n}\frac{\partial}{\partial x}p_{nn'}(x)\right) + V_n(x)\delta_{nn'}\right] F_{n'}(x)$$
$$= EF_n(x), \qquad (38)$$

where $\delta_{n<n'} = 1$ for $n < n'$ and zero otherwise, $n, n' \in A$ and all parameters are stepwise constant with the bulk value in each material. Note that for our setup $p_{nn} = 0$ as the periodic functions are either even or odd. The fact that the parameters are stepwise constant give rise to the interface boundary conditions:

$$F_n(x) \text{ and } \sum_{n'}\left[\frac{\hbar^2}{2m}\left(\gamma_{nn'}(x)\frac{\partial}{\partial x}\right) + i\frac{\hbar}{m}\delta_{n'<n}p_{nn'}(x)\right]F_{n'}(x) \qquad (39)$$

continuous at the interface. Our two band model for a heterostructure is then given by:

$$\begin{pmatrix} -\frac{\hbar^2}{2m}\frac{\partial}{\partial x}\gamma_{22}(x)\frac{\partial}{\partial x} + V_2(x) & -i\frac{\hbar}{m}p_{23}(x)\frac{\partial}{\partial x} \\ -i\frac{\hbar}{m}\frac{\partial}{\partial x}p_{32}(x) & -\frac{\hbar^2}{2m}\frac{\partial}{\partial x}\gamma_{33}(x)\frac{\partial}{\partial x} + V_3(x) \end{pmatrix}\begin{pmatrix} F_2(x) \\ F_3(x) \end{pmatrix} = E\begin{pmatrix} F_2(x) \\ F_3(x) \end{pmatrix}, \quad (40)$$

where V_2 and V_3 are given by the zone-center energies. In Fig. 5 we show a sketch of γ_{22} (the other parameters have a similar x dependence).

It turns out that in some cases the solutions to this kind of multiband equations are completely incorrect solutions in terms of the original problem (even in the cases where
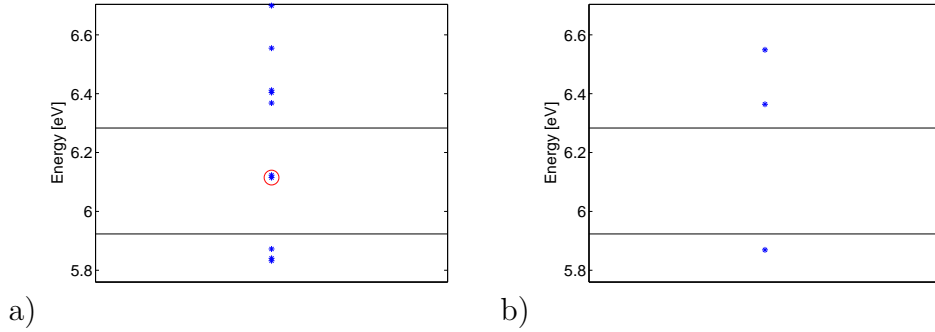
Figure 6: The bound states (the energies in the band gap of the barrier material) for a heterostructure consisting of 20 well and 20 barrier periods. The solid lines show the location of the bulk zone center energies E_{20} and E_{30} of the well material. The barrier potential is given by $V_{b0} = 0$ eV, $V_b = 5$ eV, the well potential is given by $V_{w0} = 0$ eV, $V_w = 3$ eV and $a = 5$ Å. a) The energies calculated using the heuristic two band model. b) The correct energies.

more accurate interface boundary conditions are used). In Fig. 6a) the energy spectrum is shown for a specific example. In between the solid lines is the band gap for the well material, i.e., the region in between bulk zone center energies E_{20} and E_{30}. We do not expect to see solutions in the band gap, so this suggests that the energies highlighted by a circle are incorrect. In order to check that these solutions are wrong indeed, we have carried out calculations for the case where a finite but large number of periodic functions have been used without treating the rest as remote bands, that is we have solved Eq. (14) including a large but finite U_n set. We have checked the accuracy of this approach by doubling the number of U_n states and comparing the eigen energies. It turns out that with a choice of the 10 lowest (in terms of energy) U_n, the error in the energies of interest is less than 0.1% (we refer further to these values, obtained with sufficient accuracy, as correct). The correct eigen energies are shown in Fig. 6b). From the two figures it is clear that the energies with a circle around are incorrect solutions. These solutions are known as spurious solutions as they have nothing to do with the original problem, although they are correct solutions to the multiband equation.

Our model is, in reality, over-specified. Indeed, the two band model (Eq. (40)) together with periodic boundary conditions and interface boundary conditions (Eq. (39)) result in 8 linear independent equations for the 8 unknown coefficients of the general solutions (4 general solutions in each material region). However, we also have the requirement that the Fourier expansion should be restricted to small k components. It is this last requirement which is not satisfied for the spurious solutions. In Fig. 7 we show the envelope function F_2 and its Fourier coefficients. We see that the major Fourier components are outside the first Brillouin zone. There are two separate issues here. First, from the exact envelope function theory we have the requirement that the Fourier expansion of the envelope function should be restricted to the first Brillouin zone to ensure uniqueness. This is not a major problem, however, as relaxing uniqueness requirements has been discussed in the literature, see [5]. Second, the assumption that $\hat{H}^1$ is small relies heavily on the assumption that only small k components of the envelope functions are non zero. This can be seen from the bulk expression (Eq. (31)) that is used to derive the differential equations for each separate material (the
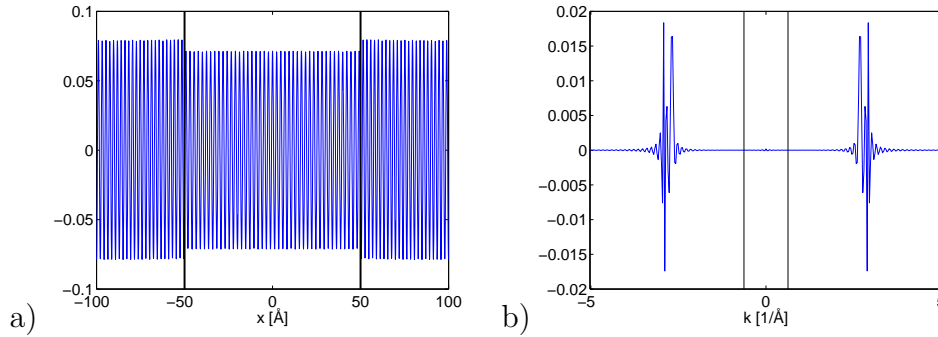
Figure 7: a) The real part of the envelope function F_2 (the imaginary part is zero). The solid black lines show the location of the interfaces. b) The real part of the Fourier coefficients of the F_2 (the imaginary part is zero), the solid lines show the boundary of the first Brillouin zone. The same parameters as in Fig. 6 have been used.

first and second terms grow quadratically and linearly with k, respectively). So if we have non-zero components for large k values the procedure used to derive multiband equations breaks down. The reason why the spurious solutions appear is that large k components are needed to satisfy the interface boundary conditions. So the problem with spurious solutions is that what would normally be considered a complete set of interface boundary conditions, i.e., $2N$ boundary conditions for a N band model, results in an over-specified problem, hence a reduced set of interface boundary conditions is needed. For approaches along these lines see, e.g. [29, 17].

Another way of getting around this problem is to reformulate the set of coupled equations in k space and to restrict the problem to the first Brillouin zone (or in some cases to a smaller region in k space, see [40]). In order to implement this idea, we expand the solutions in plane waves and make a cut-off beyond a small neighborhood of $k = 0$, see e.g. [40]. In table 1 we show the energy spectrum found using this approach together with both the correct energy spectrum and the energy spectrum found using the two band model. We see that energies found using the cut-off approach have an error of less than 0.1% compared to the correct energies. This shows that the present approach combined with plane wave cut-off removes the spurious solutions and gives quite accurate results. In Fig. 8a) we show the correct wave function together with the wave function found using the two band model with plane wave cut-off. The wave function of the two band model is given by:

$$\psi_{TwoBand}(x) = \sum_{n=2}^{3} F_n(x)\big[U_{n0,b}(x)(1 - \theta_h(x)) + \theta_h(x)U_{n0,w}(x)\big], \qquad (41)$$

where $U_{n0,b}(x)$ is the zone-center solutions for the barrier and $U_{n0,w}(x)$ is the zone-center solutions for the well. That is, we have taken into account that the periodic bases are different in the well and the barrier. The correct wave function is given by:

$$\psi_{Correct}(x) = \sum_{n=1}^{N} F_n(x)U_{n0,b}(x), \qquad (42)$$

where N is the number of periodic solutions included in the calculations. From Fig. 8a) it is hard to see any difference between the two solutions. Hence, in order to quantify the error

Exact	Two Band	Two Band with Cut-Off
	5.7292	
	5.8325	
	5.8405	
5.8690	5.8723	5.8723
	6.1151	
	6.1229	
6.3643	6.3681	6.3682
	6.4042	
	6.4115	
6.5501	6.5546	6.5546
	6.6995	
	6.7062	

Table 1: The energies of the bound states. All energies are in eV. The same parameters as in Fig. 6 have been used.
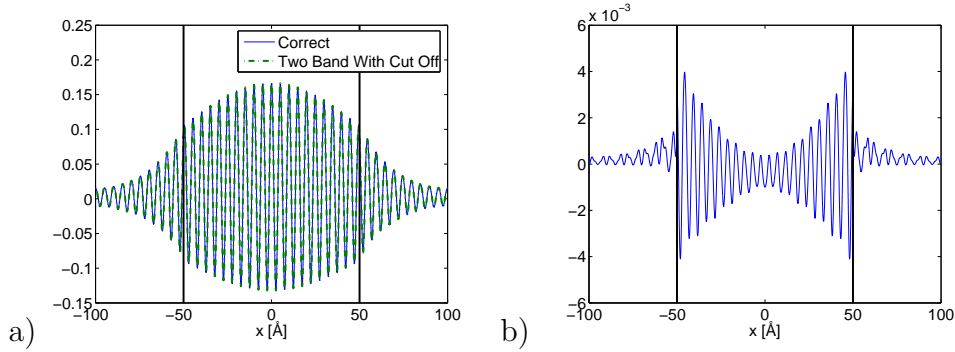
Figure 8: a) The wave function found using the exact approach (20 bands included) together with the wave function found using the two band model with plane wave cut-off. b) The difference between the two wave functions. The same parameters as in Fig. 6 have been used.

introduced by using the two band model with cut-off we also show the difference between the two (Fig. 8b)). These figures show that the wave function too is well captured by the two band model with plane wave cut-off. We also note that the difference between the two solutions is largest close to the interfaces. We have made no attempt to model the interface more accurately, so this is not surprising. Using a more correct procedure to model the interface would result in increased accuracy of the two band wave function around the interfaces.

We point out that by using the cut-off approach we are actually solving a slightly different problem compared to the original two band differential equation (Eq. 40). This is most easily seen by noting that the original interface boundary conditions are not satisfied anymore as the envelope functions within the cut-off approach are smooth and the interface boundary conditions give rise to discontinuities in the first derivative of the envelope functions. The ordering of the material dependent parameters, i.e., the interface boundary conditions, is still an issue, however, as different orderings will result in different k space equations. For

example, a term like

$$-\frac{\hbar^2}{2m}\frac{\partial}{\partial x}\gamma_{22}(x)\frac{\partial}{\partial x} \tag{43}$$

gives in k space rise to

$$\frac{\hbar^2}{2m}k\tilde{\gamma}_{22}(k-k')k', \tag{44}$$

and a term like

$$-\frac{\hbar^2}{2m}\gamma_{22}(x)\frac{\partial^2}{\partial x^2} \tag{45}$$

gives in k space rise to

$$\frac{\hbar^2}{2m}\tilde{\gamma}_{22}(k-k')k'k'. \tag{46}$$

A disadvantage of using plane wave expansions is that the resulting matrix eigenvalue problem is a problem where most of the elements of the matrix will be non-zero, as opposed to local approaches, such as finite element methods, which give rise to sparse problems. From a computational point of view, it is a concern because the full problem becomes more computationally demanding and hard to parallelize.

Another issue in working with plane waves with cut-off is that it is not obvious how to reduce the complexity of a problem using symmetries of the system. For example, if we have a three dimensional cylindrically symmetric problem, it is not obvious how to use this symmetry and at the same time to restrict the Fourier component to small k. This latter issue can be resolved and we do this in the next section.

4   Reduction of 3D models for nanostructures with cylindrical symmetry

In this section we consider three dimensional problems with cylindrical symmetry. The theory of Section 3 can easily be extended to three dimensions, see [4]. The focus of this section is on how to reduce the problem to a two dimensional problem and at the same time to ensure that the envelope functions are restricted to small k components. To simplify matters we choose to use the one band model for a cubic heterostructure:

$$\hat{H}\psi = [-\langle\nabla, A(\vec{r})\nabla\rangle + V(\vec{r})]\psi(\vec{r}) = E\psi(\vec{r}), \tag{47}$$

where $A(\vec{r}) = \frac{\hbar^2}{2m^*(\vec{r})}$, m^* is the effective mass, V is the effective potential (the conduction band edge), ∇ is the gradient. The effective mass is, in terms of the γ parameters of section 3.1, given by $1/m^* = \gamma_{SS}/m$, where S denotes the periodic zone-center solution for the condution band. The gradient of f is defined by:

$$\langle\vec{v}, \nabla f\rangle = D_{\vec{v}}f, \tag{48}$$

where $\langle\cdot, \cdot\rangle$ is the Euclidean inner product in $\mathbb{R}^3$. The problem is cylindrically symmetric as long as the effective mass m^*, the effective potential V and the domain of our system Ω are cylindrically symmetric. For simplicity we assume that $\Omega = \mathbb{R}^3$. We are looking for solutions in the form:

$$\psi(\vec{r}) = \int_{\Omega_k}\hat{\psi}(\vec{k})e^{i\langle\vec{k},\vec{r}\rangle}d^3k, \tag{49}$$

where Ω_k is a small neighborhood of $\vec{k} = 0$ to be defined later (it needs to reflect the cylindrical symmetry). Using

$$\nabla e^{i\langle \vec{k}, \vec{r}\rangle} = i\vec{k}e^{i\langle \vec{k}, \vec{r}\rangle}, \tag{50}$$

we can reformulate the one band model in k space as follows:

$$\int_{\Omega_k} [\langle \vec{k}', \hat{A}(\vec{k}', \vec{k})\vec{k}\rangle + \hat{V}(\vec{k}', \vec{k})]\hat{\psi}(\vec{k})d^3k = E\hat{\psi}(\vec{k}'), \tag{51}$$

where

$$\hat{A}(\vec{k}', \vec{k}) = \frac{1}{(2\pi)^3}\int_\Omega A(\vec{r})e^{i\langle \vec{k}-\vec{k}', \vec{r}\rangle}d^3r \text{ and } \hat{V}(\vec{k}', \vec{k}) = \frac{1}{(2\pi)^3}\int_\Omega V(\vec{r})e^{i\langle \vec{k}-\vec{k}', \vec{r}\rangle}d^3r. \tag{52}$$

Due to the cylindrical symmetry we know that

$$[\hat{H}, \hat{S}_\theta] = 0, \tag{53}$$

where $[\cdot, \cdot]$ is the commutator, $\hat{S}_\theta f(\vec{r}) = f(S_\theta\vec{r})$ for any function f and S_θ is the operator that rotates $\mathbb{R}^3$ by the angle θ around the symmetry axis. Choosing the Cartesian coordinates ($\vec{r} = (x, y, z)$) where the third axis points along the symmetry axis, we have:

$$S_\theta = \begin{pmatrix} \cos(\theta) & -\sin(\theta) & 0 \\ \sin(\theta) & \cos(\theta) & 0 \\ 0 & 0 & 1 \end{pmatrix}. \tag{54}$$

Because of the commutation relation (53) we can find wave functions ψ which are simultaneous eigen solutions of $\hat{S}_\theta$, i.e., we can find solutions ψ_l so that:

$$\hat{S}_\theta\psi_l = e^{il\theta}\psi_l, \tag{55}$$

where l is an integer. This can be verified by differentiating the eigenvalue problem $\hat{S}_\theta\psi = \lambda_\theta\psi$ with respect to θ, evaluating it at $\theta = 0$, and using the periodicity condition $S_\theta = S_{\theta+2\pi}$. Using the Fourier expansion we have:

$$\begin{aligned} e^{il\theta}\psi_l(\vec{r}) &= \hat{S}_\theta\psi_l(\vec{r}) \\ &= \psi_l(S_\theta\vec{r}) \\ &= \int_{\Omega_k}\hat{\psi}_l(\vec{k})e^{i\langle \vec{k}, S_\theta\vec{r}\rangle}d^3k \\ &= \int_{\Omega_k}\hat{\psi}_l(\vec{k})e^{i\langle S_{-\theta}\vec{k}, \vec{r}\rangle}d^3k \\ &= \int_{\Omega_k}\hat{\psi}_l(S_\theta\vec{k})e^{i\langle \vec{k}, \vec{r}\rangle}d^3k. \end{aligned} \tag{56}$$

From this it is easily seen that:

$$e^{il\theta}\hat{\psi}_l(\vec{k}) = \hat{\psi}_l(S_\theta\vec{k}). \tag{57}$$

This equation has the solution:

$$\hat{\psi}_l(\vec{k}) = e^{il\theta_k}\tilde{\psi}(k, k_z), \tag{58}$$

where

$$k_x = k\cos(\theta_k) \text{ and } k_y = k\sin(\theta_k). \tag{59}$$

Using cylindrical coordinates

$$x = r\cos(\theta_r) \text{ and } y = r\sin(\theta_r) \tag{60}$$

and using the fact that A is a function of r and z only we find:

$$
\begin{aligned}
\hat{A}(\vec{k}', \vec{k}) &= \frac{1}{(2\pi)^3} \int A(r,z) e^{i(kr\cos(\theta_k - \theta_r) - k'r\cos(\theta_{k'} - \theta_r) + (k_z - k_z')z)} r\,dr\,d\theta_r\,dz \\
&= \frac{1}{(2\pi)^3} \int A(r,z) \sum_{n,n'} (i)^{n+n'} J_n(kr) J_{n'}(-k'r) e^{in(\theta_k - \theta_r)} e^{-in'(\theta_{k'} - \theta_r)} e^{i(k_z - k_z')z} r\,dr\,d\theta_r\,dz \\
&= \frac{1}{(2\pi)^3} \int A(r,z) \sum_{n,n'} (i)^{n+n'} (-1)^{n'} J_n(kr) J_{n'}(k'r) e^{i(n\theta_k - n'\theta_{k'})} e^{i(n'-n)\theta_r} e^{i(k_z - k_z')z} r\,dr\,d\theta_r\,dz \\
&= \frac{1}{(2\pi)^2} \int A(r,z) \sum_{n} J_n(kr) J_n(k'r) e^{in(\theta_k - \theta_{k'})} e^{i(k_z - k_z')z} r\,dr\,dz,
\end{aligned}
\tag{61}
$$

where we have used that:

$$e^{ix\cos(\phi)} = \sum_n i^n J_n(x) e^{i\phi n}, \tag{62}$$

and the domain of integration is $0 \le r < r_{max}(z)$, $z_{min} < z < z_{max}$ and $0 \le \theta < 2\pi$. Here z_{min}, z_{max} and $r_{max}(z)$ are determined by Ω. In the case where $\Omega = \mathbb{R}^3$ we have $z_{min} = -\infty$, $z_{max} = \infty$ and $r_{max}(z) = \infty$. The same arguments apply to $\hat{V}$:

$$\hat{V}(\vec{k}', \vec{k}) = \frac{1}{(2\pi)^2} \int V(r,z) \sum_n J_n(kr) J_n(k'r) e^{in(\theta_k - \theta_{k'})} e^{i(k_z - k_z')z} r\,dr\,dz. \tag{63}$$

We are now in a position to integrate out all angle dependent terms in the one band model, Eq. (51). Assuming that the region in k space Ω_k is given by $k_{z,min} < k_z < k_{z,max}$, $0 \le k < k_{max}$ and $0 \le \theta_k < 2\pi$ we get:

$$
\begin{aligned}
2\pi E\tilde{\psi}(k', k_z') &= \int \big[\hat{A}(\vec{k}', \vec{k})(kk'\cos(\theta_k' - \theta_k) + k_z'k_z)\big] e^{il\theta_k} \tilde{\psi}(k, k_z) e^{-il\theta_{k'}} k\,dk\,d\theta_k\,dk_z\,d\theta_{k'} \\
&\quad + \int \hat{V}(\vec{k}', \vec{k}) e^{il\theta_k} \tilde{\psi}(k, k_z) e^{-il\theta_{k'}} k\,dk\,d\theta_k\,dk_z\,d\theta_{k'} \\
&= \frac{1}{(2\pi)^2} \int A(r,z) \sum_n J_n(kr) J_n(k'r) e^{in(\theta_k - \theta_{k'})} e^{i(k_z - k_z')z} r \\
&\quad \times \big[kk'\cos(\theta_{k'} - \theta_k) + k_z'k_z\big] e^{il\theta_k} \tilde{\psi}(k, k_z) e^{-il\theta_{k'}} k\,dr\,dz\,dk\,d\theta_k\,dk_z\,d\theta_{k'} \\
&\quad + \frac{1}{(2\pi)^2} \int V(r,z) \sum_n J_n(kr) J_n(k'r) e^{in(\theta_k - \theta_{k'})} e^{i(k_z - k_z')z} r \\
&\quad \times e^{il\theta_k} \tilde{\psi}(k, k_z) e^{-il\theta_{k'}} k\,dr\,dz\,dk\,d\theta_k\,dk_z\,d\theta_{k'} \\
&= \tfrac{1}{2} \int A(r,z)(kk'\big[J_{-l-1}(kr)J_{-l-1}(k'r) + J_{-l+1}(kr)J_{-l+1}(k'r)\big) + k_z'k_z J_{-l}(kr)J_{-l}(k'r)\big] \\
&\quad \times e^{i(k_z - k_z')z} \tilde{\psi}(k, k_z) k\,r\,dr\,dz\,dk\,dk_z \\
&\quad + \int V(r,z) J_{-l}(kr) J_{-l}(k'r) e^{i(k_z - k_z')z} \tilde{\psi}(k, k_z) k\,r\,dr\,dz\,dk\,dk_z.
\end{aligned}
\tag{64}
$$

All in all, we have:

$$
\begin{aligned}
E\tilde{\psi}(k', k_z') &= \int_{k_{z,min}}^{k_{z,max}} \int_0^{k_{max}} \frac{\tilde{A}_{l+1}(k', k_z', k, k_z) + \tilde{A}_{l-1}(k', k_z', k, k_z)}{2} k' k \tilde{\psi}(k, k_z)\,dk\,dk_z \\
&\quad + \int_{k_{z,min}}^{k_{z,max}} \int_0^{k_{max}} \tilde{A}_l(k', k_z', k, k_z) k_z' k_z \tilde{\psi}(k, k_z)\,dk\,dk_z \\
&\quad + \int_{k_{z,min}}^{k_{z,max}} \int_0^{k_{max}} \tilde{V}_l(k', k_z', k, k_z) \tilde{\psi}(k, k_z)\,dk\,dk_z,
\end{aligned}
\tag{65}
$$

where

$$\tilde{A}_l(k', k_z', k, k_z) = \frac{k}{2\pi} \int_{z_{min}}^{z_{max}} \int_0^{r_{max}(z)} A(r,z) J_l(kr) J_l(k'r) e^{i(k_z - k_z')z} r\,dr\,dz, \tag{66}$$

$$\tilde{V}_l(k', k_z', k, k_z) = \frac{k}{2\pi} \int_{z_{min}}^{z_{max}} \int_0^{r_{max}(z)} V(r,z) J_l(kr) J_l(k'r) e^{i(k_z - k_z')z} r\,dr\,dz, \tag{67}$$

and we have used $J_{-l}(x) = (-1)^l J_l(x)$.

We have now reduced the problem to a two dimensional problem while ensuring that the Cartesian plane wave expansion is restricted to small $\mathbf{k}$ components. It is not surprising that the radial part should be expanded in Bessel functions as these functions are the radial solutions to the Laplace eigenvalue equation in cylindrical coordinates. It is, however, not obvious that restricting to small k components of the Bessel functions (and k_z components) is equivalent to the restriction to small $\mathbf{k}$ components.

5   Conclusions and future directions

In this paper we focused on a long standing problem in the application of the multiband effective mass theory to low dimensional nanostructures that manifests itself in the appearance of non-physical spurious solutions. Due to its fundamental significance and a wide range of applications in science and engineering, there have been a substantial number of attempts to resolve this problem. We reviewed some of such approaches together with available techniques for formulating interface boundary conditions for the associated model for the envelope functions. Next, based our discussion on the generalized envelope function theory, we derived multiband equations for the one dimensional case. We demonstrated that a failure to restrict the Fourier expansion of the envelope functions to small k components, which is in the heart of the multiband model derivation, may lead to spurious solutions with no physical meaning. On an example of a heterostructure, we provided details of a procedure of how such non-physical solutions can be removed and evaluated the accuracy of the results obtained. Finally, we exemplified this approach by a reduction of a three dimensional cylindrically symmetric problem to a two dimensional problem within the plane wave cut-off approach. The resulting model provides a computationally efficient framework for the analysis of cylindrical symmetric systems and details of such an analysis will be reported elsewhere. Finally, we note that an appropriate choice of the basis for our multiband model may bring further computational advantages leading to the effect of the Gibbs phenomenon being minimized while moving from the $\mathbf{k}$-space to the real physical space. The resulting systems of linear equations will be sparse, as we pointed out in Section 2, reducing further the computational cost and providing additional advantages of this methodology as compared to ab initio and atomistic techniques. This issue deserves further discussion in a separate publication.

Acknowledgments

Appendix

Any periodic lattice is completely specified by its principle lattice vectors $\mathbf{a}_1, \mathbf{a}_2$ and $\mathbf{a}_3$ defined such that any translation vector $\mathbf{R}$ (a vector connecting two lattice points) can be written as:

$$\mathbf{R} = m_1\mathbf{a}_1 + m_2\mathbf{a}_2 + m_3\mathbf{a}_3, \tag{68}$$

for some $m_1, m_2, m_3 \in \mathbb{Z}$. Based on the principle lattice vectors, the reciprocal lattice can be defined as those vectors $\mathbf{b}$ that satisfy:

$$\exp(i\mathbf{b}\mathbf{R}) = 1. \tag{69}$$

It can be shown that any reciprocal lattice vector is given by:

$$\mathbf{b} = n_1\mathbf{b}_1 + n_2\mathbf{b}_2 + n_3\mathbf{b}_3, \tag{70}$$

for some $n_1, n_2, n_3 \in \mathbb{Z}$, where $\mathbf{b}_1 = 2\pi/\Omega_0[\mathbf{a}_2 \times \mathbf{a}_3]$, $\mathbf{b}_2 = 2\pi/\Omega_0[\mathbf{a}_3 \times \mathbf{a}_1]$, $\mathbf{b}_3 = 2\pi/\Omega_0[\mathbf{a}_1 \times \mathbf{a}_2]$ and $\Omega_0 = \mathbf{a}_1[\mathbf{a}_2 \times \mathbf{a}_3]$.

There are many reasons for the construction of the reciprocal lattice. The one we focus on here is its relation to irreducible representations of the translational group related to the translation vectors $\mathbf{R}$ (that is the translational symmetry of the system). It can be shown that any irreducible representation of the translational group is completely determined by $\lambda_1 = \exp(-i\mathbf{k}\mathbf{a}_1), \lambda_2 = \exp(-i\mathbf{k}\mathbf{a}_2), \lambda_3 = \exp(-i\mathbf{k}\mathbf{a}_3)$ where vector $\mathbf{k}$ is determined up to an arbitrary reciprocal lattice vector, see [2]. The ambiguity in $\mathbf{k}$ can be removed by restricting to the first Brillouin zone (the Wigner-Seitz cell of the reciprocal lattice).

References

[1] G. Bastard Wave mechanics applied to semiconductor heterostructures. New York: Halsted Press (a division of John Wiley & Sons), 1988.

[2] G.L. Bir, G.E. Pikus Symmetry and strain-induced effects in semiconductors. New York: Wiley, 1974.

[3] M. G. Burt. An exact formulation of the envelope function method for the determination of electronic states in semiconductor microstructure. *Semicond. Sci. Technol.*, 3:739, 1988.

[4] M. G. Burt. The justification for applying effective-mass approximation to microstructures. *J. Phys. Condens. Matter*, 4:6651, 1992.

[5] M. G. Burt. Resolution of the out-of-zone solution problem in envelope-function theory. *Superlatt. Microstruct.*, 23:531, 1998.

[6] M.G. Burt, Fundamentals of envelope function theory for electronic states and photonic modes in nanostructures, *J. Phys.: Condens. Matter*, 11, R53-R83, 1999.

[7] B. Chen, M. Lazzouni, and L. R. Ram-Mohan. Diagonal representation for the transfer-matrix method for obtaining electronic energy levels in layered semiconductor heterostructures. *Phys. Rev. B*, 45(3):1204–1212, Jan 1992.

[8] J. P. Cuypers and W. van Haeringen. Connection rules for envelope functions at semiconductor-heterostructure interfaces. *Phys. Rev. B*, 47(16):10310–10318, Apr 1993.

[9] J. H. Davies The physics of low-dimensional semiconductors. Cambridge: Cambridge University Press, 1998.

[10] E. Ertekin, P.A. Greaney, and D.C. Chrzan, Equilibrium limits of coherency in strained nanowire heterostructures, *J. of Applied Physics*, 97, 114325, 2005.

[11] B. A. Foreman, Effective-mass Hamiltonian and boundary conditions for the valence bands of semiconductor microstructures, *Physical Review B*, 48 (7), 4964–4967, 1993.

[12] B. A. Foreman. Elimination of spurious solutions from eight-band k·p theory. *Phys. Rev. B*, 56:R12748, 1997.

[13] B. A. Foreman. Connection rules versus differential equations for envelope functions in abrupt heterostructures. *Phys. Rev. Lett.*, 80(17):3823–3826, Apr 1998.

[14] B. A. Foreman. Choosing a basis that eliminates spurious solutions in k·p theory. *Physical Review B*, 75 (23): 235331, 2007.

[15] B. A. Foreman. First-principles envelope-function theory for lattice-matched semiconductor heterostructures. *Physical Review B (Condensed Matter and Materials Physics)*, 72(16):165345, 2005.

[16] B. A. Foreman. Envelope-function formalism for electrons in abrupt heterostructures with material-dependent basis functions. *Phys. Rev. B*, 54:1909, 1996.

[17] M. J. Godfrey and A. M. Malik. Boundary conditions and spurious solutions in envelope-function theory. *Phys. Rev, B*, 53:16504, 1996.

[18] K.I. Kolokolov, J. Li, and C.Z. Ning, $k \cdot p$ Hamiltonian without spurious-state solutions, *Physical Review B*, 68, 161308(R), 2003.

[19] B. Lassen B, L. C. Lew Yan Voon, M Willatzen, R. V. N. Melnik. Exact envelope-function theory versus symmetrized Hamiltonian for quantum wires: a comparison. Solid State Communications. 2004; 132(3-4): 141–149.

[20] B. Lassen, M. Willatzen, R. Melnik and L. C. Lew Yan Voon, A General Treatment of Deformation Effects in Hamiltonians for Inhomogeneous Crystalline Materials, *Journal of Mathematical Physics*, Vol. 46, 112102, 2005.

[21] B. Lassen, M. Willatzen, R. Melnik, and L. C. Lew Yan Voon, Electronic properties of free-standing InP and InAs nanowires, *J. Mat. Res.* 21 (11), 2927-2935, 2006.

[22] B. Lassen, M. Willatzen, R. Melnik and L. C. Lew Yan Voon, Spurious solutions and boundary conditions in $k \cdot p$ theory, *Proc. 28th Int. Conf. Phys. Semi., AIP Conf. Proc.* 893, 993-994, 2007.

[23] S. Lee, F. Oyafuso, P. von Allmen, and G. Klimeck, Boundary conditions for the electronic structure of finite-extent, embedded semiconductor nanostructures, *Physical Review B*, 69 (4): 045316, 2004.

[24] J.M. Luttinger and W. Kohn, Motion of electrons and holes in perturbed periodic fields, *Physical Review*, 97 (4), 869–883, 1955.

[25] R. V. N. Melnik, M. Willatzen Bandstructures of conical quantum dots with wetting layers. Nanotechnology, 15 (1), 1–8, 2004.

[26] R. Melnik and R. Mahapatra, Coupled effects in quantum dot nanostructures with nonlinear strain and bridging modelling scales, *Computers & Structures*, 85 (11-14), 698-711, 2007.

[27] R. Melnik, Multiple Scales and Coupled Effects in Modelling Low Dimensional Semiconductor Nanostructures: Between Atomistic and Continuum Worlds, *Encyclopedia of Complexity and Systems Science*, Springer, to appear.

[28] A. T. Meney, Besire Gonul, and E. P. O'Reilly. Evaluation of various approximations used in the envelope-function method. *Phys. Rev. B*, 50:10893, 1994.

[29] A. V. Rodina, A. Yu Alekseev, Al. L. Elfros, M. Rosen, and B. K. Meyer. General boundary conditions for the envelope fnuction in the multiband k·p model. *Phys. Rev. B*, 65:125302–1, 2002.

[30] A.V. Rodina and A.Y. Alekseev, Least-action principle for envelope functions in abrupt heterostructures, *Physical Review B*, 73, 115312, 2006.

[31] J. Singh Physics of semiconductors and their heterostructures. New York: McGraw-Hill, 1993.

[32] J.C. Slater, Electrons in perturbed periodic lattices, *Physical Review*, 76 (11), 1592–1601, 1949.

[33] F. Szmulowicz, Solution to spurious bands and spurious real solutions in the envelope-function approximation, *Physical Review B*, 71, 245117, 2005.

[34] I.V. Tokatly, A.G. Tsibizov, and A.A. Gorbatsevich, Interface electronic states and boundary conditions for envelope functions, *Physical Review B*, 65, 165328, 2002.

[35] R. G. Veprek, S. Steiger, and B. Witzigmann, Ellipticity and the spurious solution problem of $k \cdot p$ envelope equations, *Physical Review B*, 76 (16): 165320, 2007.

[36] S. R. White and L. J. Sham, Electronic properties of flat-band semiconductor heterostructures, *Physical Review Letters*, 47, 879, 1981.

[37] M. Willatzen, R. V. N. Melnik, C. Galeriu, and L. C. Lew Yan Voon Quantum confinement phenomena in nanowire superlattice structures. Mathematics and Computers in Simulation. 2004; 65(4-5): 385–397.

[38] M. Willatzen, B. Lassen, L.C. Lew Yan Voon, and R.V.N Melnik, Dynamic coupling of piezoelectric effects, spontaneous polarization, and strain in lattice-mismatched semiconductor quantum-well heterostructures, *Journal of Applied Physics*, 100, 024302, 2006.

[39] R. Winkler and U. Rössler. General approach to the envelope-function approximation based on a quadrature method. *Phys. Rev. B*, 48(12):8918–8927, Sep 1993.

[40] W. Yang and Kai Chang. Origin and elimination of spurious solutions of the eight-band k·p theory. *Phys. Rev. B*, 72:233309, 2005.